Inorganic Chemistry

Article

pubs.acs.org/IC

Synthesis, Structural Elucidation, and Application of a Pyrazolylpyridine–Molybdenum Oxide Composite as a Heterogeneous Catalyst for Olefin Epoxidation

Sónia Figueiredo,[†] Ana C. Gomes,[‡] Patrícia Neves,[‡] Tatiana R. Amarante,[‡] Filipe A. Almeida Paz,*[,‡] Rosário Soares,[§] André D. Lopes,[†] Anabela A. Valente,[‡] Martyn Pillinger,[‡] and Isabel S. Gonçalves*[,‡]

[†]Faculty of Science and Technology, Department of Chemistry, Biochemistry and Pharmacy, Centro de Investigação em Química do Algarve, University of the Algarve, Campus de Gambelas, 8005-136 Faro, Portugal

[‡]Department of Chemistry, CICECO, University of Aveiro, 3810-193 Aveiro, Portugal

[§]Central Analytical Laboratory, University of Aveiro, 3810-193 Aveiro, Portugal

Supporting Information

ABSTRACT: The reaction of $[MoO_2Cl_2(pypzEA)]$ (**1**) (pypzEA = ethyl[3-(pyridin-2-yl)-1*H*-pyrazol-1-yl]acetate) with water in a Teflon-lined stainless steel autoclave (100 °C) or in an open reflux system leads to the isolation of the molybdenum oxide/pyrazolylpyridine composite material $[Mo_2O_6(HpypzA)]$ (**2**; HpypzA = [3-(pyridinium-2-yl)-1*H*-pyrazol-1-yl]-acetate). The solid state structure of **2** was solved through single crystal and powder X-ray diffraction analyses in conjunction with information derived from FT-IR and ^{13}C CP MAS NMR spectroscopies and elemental analyses. In the asymmetric unit of **2**, two crystallographically distinct Mo^{6+} centers are bridged by a *syn,syn*-carboxylate group of HpypzA. The periodic repetition of these units along the *a* axis of the unit cell leads to the formation of a one-dimensional composite polymer, $_\infty{}^1[Mo_2O_6(HpypzA)]$. The outstretched pyrazolylpyridine groups of adjacent polymers interdigitate to form a zipper-like motif, generating strong onset $\pi-\pi$ contacts between adjacent rings of coordinated HpypzA molecules. The composite oxide **2** is a stable heterogeneous catalyst for liquid-phase olefin epoxidation.

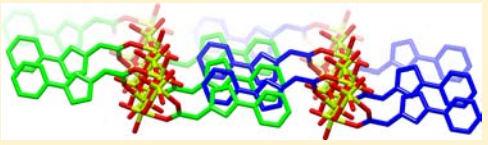

INTRODUCTION

Molybdenum oxide-based organic–inorganic composite materials have been of interest for some time due to their potential application in many fields, such as catalysis, sorption, electrical conductivity, magnetism, electronics, and optical materials.[1,2] In the design of new materials, researchers have focused on using the organic component to alter the inorganic oxide microstructure. In this way, a very large family of materials has been prepared with structures that comprise one-dimensional (1D) chains, two-dimensional (2D) sheets, and three-dimensional (3D) networks, as well as discrete clusters. One class of materials that has attracted particular attention is that in which the organic component is an organonitrogen compound. Zubieta and co-workers identified three subclasses for these materials based on the role of the organic molecule as a charge-compensating organoammonium cation, as a ligand bonded to a secondary transition-metal cation, and as a ligand bonded directly to a molybdenum site of the oxide substructure.[1] Some examples of the ligands used are 2,2′-bipyridine (2,2′-bipy),[2a−c] 4,4′-bipyridine,[2d−f] 2,2′-dipyridylamine,[2g] 4,4′-dipyridylamine,[2h,i] 1,10-phenanthroline,[2j] 2-(1*H*-pyrazol-3-yl)pyridine (pzpy),[2k] pyrazine,[2l] 2,4,6-tripyridyltriazine,[2m] 1,2,3-triazole,[2n] and 1,2,4-triazoles.[2o]

The conventional preparation of molybdenum oxide/organic composites involves hydrothermal treatment at 160–200 °C of aqueous solutions containing the organic molecule and the molybdenum source, which is usually Na_2MoO_4, MoO_3, or $(NH_4)_6Mo_7O_{24}$. This method frequently affords crystals suitable for X-ray diffraction. On the other hand, the yields can be low, and mixtures of phases are sometimes obtained that require mechanical separation. We have been exploring alternative approaches that use stable and easily storable mononuclear molybdenum complexes as single-source molecular precursors. Thus, the oxidative decarbonylation of the tetracarbonyl complexes $[Mo(CO)_4(L)]$ (L = 2,2′-bipy, pzpy) by reaction with *tert*-butylhydroperoxide (TBHP) at room temperature gives microcrystalline $[MoO_3(2,2'\text{-bipy})]$ and $[Mo_4O_{12}(pzpy)_4]$ in excellent yields.[3,4] In these compounds, $\{MoO_4N_2\}$ octahedra share corners to form 1D chains in the former and tetranuclear square-type species in the latter. The structure-directing influence of the organodiamines is well illustrated by the fact that the same compounds are obtained when mixtures of MoO_3, the organic ligand, and water are hydrothermally treated at 160 °C.[2a,k] Preliminary investigations have shown that these materials are active, selective, and stable catalysts for the epoxidation of *cis*-cyclooctene, used as a model substrate.[3,4]

The hydrolysis and condensation of complexes of the type $[MoO_2Cl_2L]$ is another potentially interesting route to molybdenum oxide/organic composites. This approach borrows concepts from sol–gel chemistry, i.e., hydrolysis of a metal

Received: June 29, 2012
Published: July 25, 2012

   dx.doi.org/10.1021/ic301405r | *Inorg. Chem.* 2012, 51, 8629–8635

chloride bond in a molecular precursor to give reactive M−OH species that condense through oxolation and/or olation reactions to give metal-oxo clusters, oligomers, and polymers assembled via M−O−M and/or M−OH−M bridges.[5] We found that the reaction of $[MoO_2Cl_2(2,2'\text{-bipy})]$ with water at 100−120 °C gives the hybrid molybdenum oxide/bipyridine material $\{[MoO_3(2,2'\text{-bipy})][MoO_3(H_2O)]\}_n$ with a crystal structure containing 1D inorganic and inorganic/organic composite polymers linked by O−H···O hydrogen bonds.[6] A similar treatment of $[MoO_2Cl_2(\text{di-}t\text{Bu-bipy})]$ (di-*t*Bu-bipy = 4,4′-di-*tert*-butyl-2,2′-bipyridine) gives octanuclear $[Mo_8O_{22}(OH)_4(\text{di-}t\text{Bu-bipy})_4]$ with a structure that comprises a purely inorganic core, $Mo_4(\mu_3\text{-}OH)_2O_8(\mu_2\text{-}O)_2$, attached to two peripheral oxo-bridged binuclear units, $Mo_2O_4(\mu_2\text{-}O)_2(OH)(\text{di-}t\text{Bu-bipy})$.[7] The octanuclear complex exhibited promising performance as a catalyst for the epoxidation of bioderived olefins.

The complex $[MoO_2Cl_2(\text{pypzEA})]$ (**1**) (pypzEA = ethyl[3-(pyridin-2-yl)-1*H*-pyrazol-1-yl]acetate) is an effective homogeneous catalyst for the epoxidation of olefins.[8] Here, we report that upon treatment of **1** with water, sequential hydrolysis of the Mo−Cl bonds and the ester group in the organic ligand results in the formation of the inorganic/organic composite oxide $[Mo_2O_6(\text{HpypzA})]$ (**2**; HpypzA = [3-(pyridinium-2-yl)-1*H*-pyrazol-1-yl]acetate), the structure of which has been determined through a combination of X-ray diffraction techniques. The coordination mode of the pyrazolylpyridine ligand switches from N,N-bidentate in **1** to *syn,syn* O,O-bidentate bridging in **2**. We chose the molybdenum-catalyzed epoxidation of cyclooctene as a model reaction to assess the catalytic properties of **2** and found that it exhibits catalytic activity under mild reaction conditions and behaves as a stable heterogeneous catalyst.

EXPERIMENTAL SECTION

Methods. All chemicals were purchased from Sigma-Aldrich and used as received. The complex $[MoO_2Cl_2(\text{pypzEA})]$ (**1**) was prepared as described previously.[9]

$[Mo_2O_6(\text{HpypzA})]$ (2). *Method A.* A Teflon-lined stainless steel autoclave was charged with **1** (0.50 g, 1.16 mmol) and water (20 mL) and heated in an oven at 100 °C for 19 h. The resultant pale blue solid was separated from the aqueous mother liquor (pH 1−3) by filtration; washed with water, acetone, and diethyl ether (20 mL each); vacuum-dried; and identified as **2** (0.22 g, 77%; based on Mo) by elemental analysis, FT-IR spectroscopy, and powder X-ray diffraction (PXRD).

Method B. A Schlenk tube was charged with **1** (0.50 g, 1.16 mmol) and water (20 mL), and the mixture was refluxed for 12 h under nitrogen using an external oil bath as a heating source. The resultant pale blue solid was recovered by filtration; washed with water, acetone, and diethyl ether (20 mL each); vacuum-dried; and identified as **2** (0.25 g, 88%; based on Mo) by elemental analysis, FT-IR spectroscopy, and PXRD.

Physical Data for 2. ^{13}C CP MAS NMR: δ 56.3 (NCH_2), 104.2 (C^4), 123.9 (C^8), 127.7 (C^{10}), 132.7 (C^5/C^9), 138.4 (C^{11}), 142.3 (C^3), 149.2 (C^7), 172.7 ($CH_2CO_2^-$). IR (KBr): ν 3136 (w), 3116 (w), 3063 (w), 2942 (w), 1607 (vs), 1543 (m), 1497 (w), 1481 (w), 1467 (w), 1444 (m), 1414 (s), 1333 (m), 1303 (m), 1277 (m), 1244 (m), 1228 (m), 1198 (w), 1171 (w), 1131 (w), 1095 (w), 1066 (w), 1041 (w), 1018 (w), 948 (vs), 939 (vs), 918 (s), 900 (vs), 765 (vs), 734 (w), 714 (m), 695 (w), 683 (w), 620 (s), 543 (vs, br), 482 (s), 381 (m), 350 (w), 318 (w) cm^{-1}. Raman: ν 3139 (w), 3114 (w), 3098 (w), 2976 (w), 2939 (w), 1626 (s), 1606 (m), 1540 (m), 1509 (w), 1482 (w), 1441 (w), 1406 (w), 1374 (w), 1016 (m), 958 (vs), 908 (s), 796 (m), 664 (m), 383 (w), 303 (w), 214 (vs) cm^{-1}. Elemental analysis calcd (%) for $C_{10}H_9Mo_2N_3O_8$: C, 24.46; H, 1.85; N, 8.56. Found: C, 24.60; H, 2.00; N, 8.62.

Characterization. Microanalyses for C, H, and N were performed at the Instituto de Tecnologia Química e Biológica, Oeiras, Portugal (by C. Almeida). Scanning electron microscopy (SEM) and energy dispersive X-ray spectroscopy (EDS) were performed using a Hitachi S4100 microscope operating at 25 kV. Samples were prepared by deposition on aluminum sample holders followed by carbon coating performed on an Emitech K 950 carbon evaporator.

IR spectra were recorded as KBr pellets using a Unican Mattson Mod 7000 spectrophotometer equipped with a DTGS CsI detector. Attenuated total reflectance (ATR) spectra were measured on the same instrument equipped with a Specac Golden Gate Mk II ATR accessory having a diamond top-plate and KRS-5 focusing lenses. The FT-Raman spectrum was recorded on a RFS-100 Bruker FT-Spectrometer equipped with a Nd:YAG laser with an excitation wavelength of 1064 nm.

Solid-state ^{13}C cross-polarization (CP) magic-angle spinning (MAS) NMR spectra were measured at 100.62 MHz on a wide-bore Bruker Avance 400 spectrometer (9.4 T). The spectra were acquired with a 3.5 μs 90° proton pulse, 2 ms contact time, spinning rates in the 7−11 kHz range, and 4 s recycle delays. Chemical shifts are quoted in parts per million (ppm) with respect to tetramethylsilane.

A detailed description of the X-ray diffraction studies (collection and indexation of the conventional PXRD data for $[Mo_2O_6(\text{HpypzA})]$ (**2**), structure solution from PXRD by using direct methods and by using FOX,[10] structure solution from single crystal XRD data, and the final Rietveld refinement from PXRD data) is given in the Supporting Information.

Catalytic Epoxidation Reactions. The liquid-phase catalytic epoxidation of *cis*-cyclooctene (Cy) was carried out with magnetic stirring (800 rpm) under air in closed borosilicate microreactors of 5 mL capacity, immersed in a thermostatted oil bath (55 °C). The reaction mixtures consisted of an amount of catalyst equivalent to 18 μmol of molybdenum, 1.8 mmol of Cy, and 2.75 mmol of oxidant, and in some cases 1 mL of cosolvent was added. The oxidant solutions used were 5−6 M *tert*-butylhydroperoxide in decane (denoted TBHPdec) and 70% aqueous TBHP (TBHPaq). The tested cosolvents were 1,2-dichloroethane, decane, and *n*-hexane in the case of TBHPdec as the oxidant and ethanol and water in the case of TBHPaq. All reagents and cosolvents were used as received. The Cy/catalyst/cosolvent solutions were preheated to 55 °C over 10 min (under agitation) prior to the addition of the oxidant solution, which was also preheated in a similar fashion. Zero time was taken as the instant the oxidant solution was added to the reactor.

The reaction of Cy was carried out in the presence of **2** using a predried (using $MgSO_4$) mixture of TBHPaq and DCE (1,2-dichloroethane; this system is denoted **2**/TBHPaq/DCEdry). The oxidant concentration of the TBHPaq/DCEdry mixture was confirmed by iodometric titration. The molar ratio Mo/Cy/TBHP was maintained, and the preheating of the reagents was also performed for this catalytic system.

Each reaction system contained a solid phase, which was separated after 24 h of reaction by centrifugation (3500 rpm, 10 min), thoroughly washed with *n*-hexane, and dried at 50 °C

dx.doi.org/10.1021/ic301405r | Inorg. Chem. 2012, 51, 8629−8635

Scheme 1. Synthesis of the Molybdenum Oxide/Pyrazolylpyridine Composite Material 2[a]

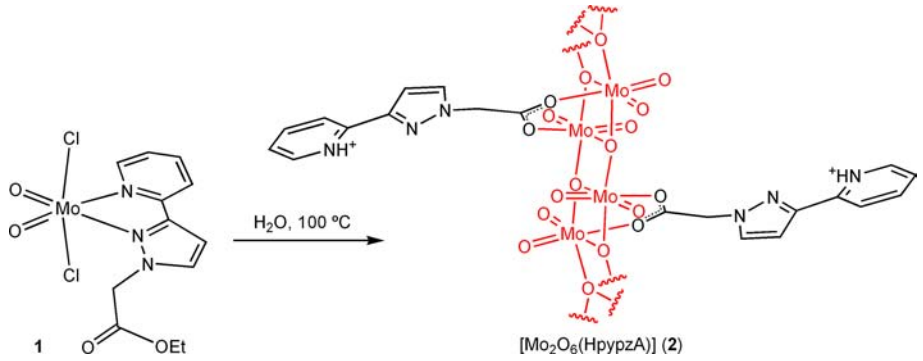

[a]A section of the purely inorganic chain is highlighted in red.

under static air, to give what is referred to throughout the discussion as "recovered solid".

The Filt_test assessment consisted of carrying out the following two experiments: (i) the reaction of Cy in the presence of catalyst for 6 h, after which time the reaction solution was filtered off at the reaction temperature (through a 0.2 μm PVDF w/GMF Whatman membrane filter), transferred into an empty, clean reactor, and left to stir for a further 18 h at 55 °C; (ii) the reaction of Cy without adding a catalyst. The increments in conversion between 6 and 24 h reaction for i and ii are denoted as ΔFiltCat and Δnone, respectively, and the increment in conversion between 6 and 24 h for the catalytic reaction under typical conditions (without filtration) is denoted as Δcat. It is considered that the catalytic reaction is heterogeneous in nature when ΔFiltCat/Δnone = 1 (Δnone > 0) and homogeneous when ΔFiltCat/Δcat = 1.

The evolution of the catalytic reactions was monitored by using a Varian 3900 GC equipped with a flame ionization detector and a DB-5 capillary column (30 m × 0.25 mm × 0.25 μm). The reaction product was identified by GC-MS (Trace GC 2000 Series Thermo Quest CE Instruments GC; Thermo Scientific DSQ II) using He as the carrier gas.

RESULTS AND DISCUSSION

Synthesis. The reaction of $[MoO_2Cl_2(pypzEA)]$ (**1**) with water was carried out either hydrothermally in a sealed Teflon-lined stainless steel digestion bomb (autogenous pressure, 100 °C, 19 h) or in an open reflux system in the air (12 h, oil bath heating). In each case, a pale blue solid was obtained, which was recovered by filtration, washed with water and organic solvents, and vacuum-dried. Practically identical elemental analysis, FT-IR, and PXRD data were obtained for both solid products, indicating that the synthesis method had no significant influence on the outcome of the reaction. Figure S1 in the Supporting Information shows representative SEM images of the microcrystalline powders obtained. EDS analyses confirmed the absence of Cl in the products. On the basis of the characterization data and the crystal structure solution described below, the product is formulated as $[Mo_2O_6(HpypzA)]$ (**2**), where HpypzA = [3-(pyridinium-2-yl)-1*H*-pyrazol-1-yl]acetate (Scheme 1).

The FT-IR spectrum of **2** displays a strong band at 765 cm^{-1} and numerous bands in the 1000−1600 cm^{-1} range assignable to the pyrazolylpyridine ligand. However, whereas complex **1** exhibits a very strong ν(CO) band at 1742 cm^{-1} for the ester group, this band is absent for **2**, and instead two strong bands are observed at 1606 and 1414 cm^{-1}, which are attributed to asymmetric and symmetric carboxylate stretching vibrations, respectively. This is in full agreement with the crystal structure solution from PXRD data (described below), which revealed the presence of HpypzA groups coordinated in a bidentate fashion to the molybdenum centers. The hydrolysis of the Mo−Cl bonds in **1** gives HCl and an acidic solution (pH 1−3), which likely promotes the acid-catalyzed hydrolysis of the ester group in pypzEA to the parent acetate and ethanol. In vibrational spectroscopic studies of acetate complexes, the frequency difference ($\Delta\nu$) between the $\nu_{asym}(CO_2^-)$ and $\nu_{sym}(CO_2^-)$ bands is often used to draw conclusions about the type of carboxylate coordination.[11] The value of $\Delta\nu$ for **2** is 192 cm^{-1}, which is in the range generally expected for bidentate bridging coordination ($\Delta\nu$ = 100−200 cm^{-1}).[11,12] As described below, the crystal structure of **2** contains edge-sharing distorted $\{MoO_6\}$ octahedra comprising three μ_3-bridging oxide groups, two terminal Mo═O groups, and one oxygen arising from a *syn*,*syn*-bridging carboxylate group of HpypzA. On the basis of this information, the IR bands observed at 900, 918, 939, and 948 cm^{-1} are assigned to ν(Mo═O), while the very strong, broad band at 544 cm^{-1} is assigned to $\nu(OMo_3)$.

The ^{13}C CP MAS NMR spectrum of **2** confirms that hydrolysis of the ester group in **1** took place during the reaction in water (Figure 1). Thus, the bands expected for the ethyl group at about 14 (CH_3) and 53 ppm (CH_2) are absent in the spectrum of **2**, while the carbonyl resonance has shifted from

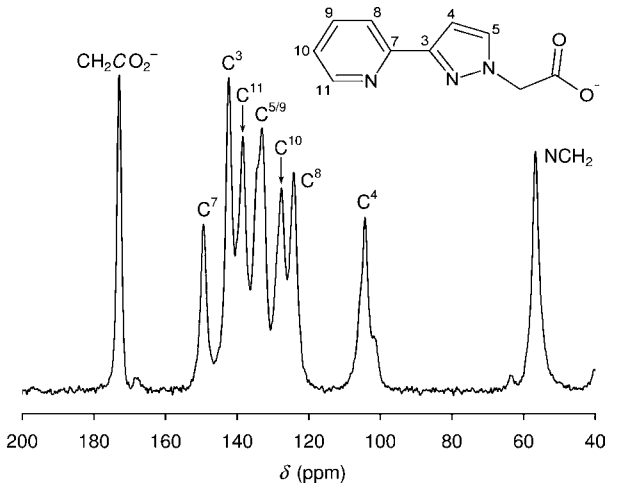

Figure 1. ^{13}C CP MAS NMR spectrum of **2**.

dx.doi.org/10.1021/ic301405r | *Inorg. Chem.* 2012, 51, 8629−8635

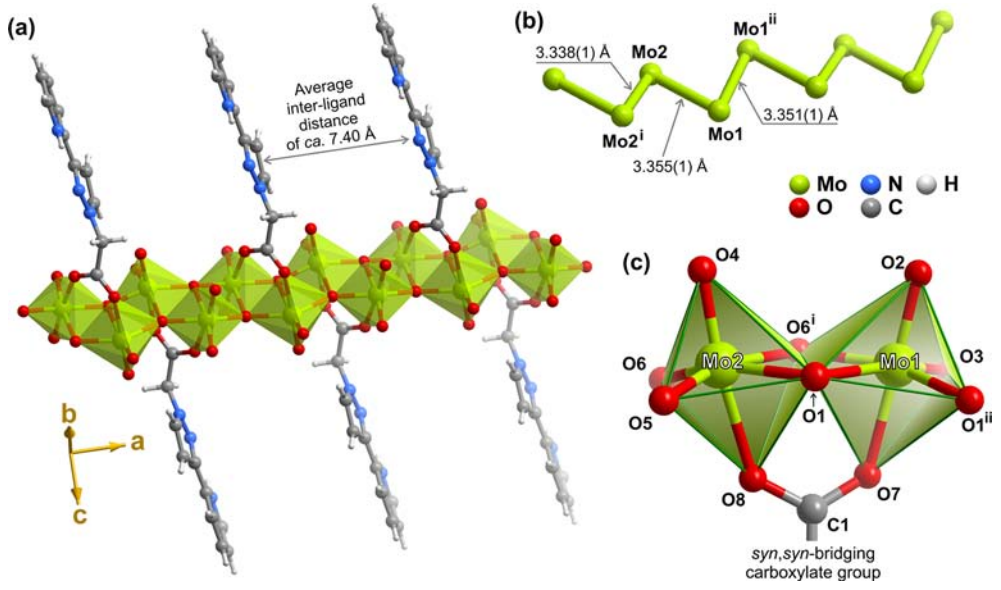

Figure 2. (a) Schematic representation of the one-dimensional $_{\infty}^{1}[Mo_2O_6(HpypzA)]$ coordination polymer present in **2**, running parallel to the *a* axis of the unit cell and composed of edge-shared $\{MoO_6\}$ distorted octahedra. (b) Magnification of the core of the Mo^{6+} oxide composite chain emphasizing the Mo···Mo intermetallic distances. (c) Portion of the composite chain emphasizing the two crystallographically independent $\{MoO_6\}$ octahedra fused together *via* the two μ_3-bridging oxygen atoms O1 and O6. The atomic labeling scheme is provided for all atoms composing the coordination polyhedra. See Table S2 for selected bond lengths and angles associated with these two coordination environments. Symmetry transformations used to generate equivalent atoms: (i) $-x, -y, 1 - z$; (ii) $1 - x, -y, 1 - z$.

167 ppm for **1** to 173 ppm for **2**. The remaining resonances can be readily assigned to the NCH_2 and pyrazolylpyridine carbons.

Crystal Structure Description. As described in the Supporting Information, the structural details of $[Mo_2O_6(HpypzA)]$ (**2**) could only be unveiled by using a complex combination of X-ray diffraction techniques and approaches, always closely complemented with the structural information derived from FT-IR and ^{13}C CP MAS NMR spectroscopies and elemental analyses. The crystal structure of **2** was ultimately refined using powder X-ray studies from laboratory data (Figure S3). The material crystallizes in the centrosymmetric triclinic space group $P\bar{1}$ (Table S1). The most striking feature is the presence of a one-dimensional inorganic/organic composite oxide polymer, $_{\infty}^{1}[Mo_2O_6(HpypzA)]$, running parallel to the *a* axis of the unit cell as depicted in Figures 2a and 3 (see also the rotational movie provided in the Supporting Information). A search in the literature and in the Cambridge Structural Database (CSD, version 5.32 with five updates)[13] reveals the existence of only a handful of somewhat related structures: $[Mo_3O_9(1,10\text{-phenanthroline})_2]_n$ described by Zhou et al.;[2j] $[MoO_3(2,2'\text{-bipy})]_n$, $[Mo_2O_6(2,2'\text{-bipy})]_n$, and $[Mo_3O_9(2,2'\text{-bipy})_2]_n$ reported by Zubieta and co-workers;[2a] $[Mo_4O_{12}(2,2'\text{-bipy})_3]_n$ described by Koo and co-workers;[2b] and $\{[MoO_3(2,2'\text{-bipy})][MoO_3(H_2O)]\}_n$, very recently described by some of us.[6] The latter structure contains a neutral and purely inorganic chain based on fused edge-shared $\{MoO_6\}$ octahedra, $_{\infty}^{1}[MoO_3(H_2O)]$, very similar to that in **2**, but the sixth coordination position is occupied by a water molecule, whereas in **2** it is occupied by an oxygen arising from the *syn,syn*-bridging carboxylate group of HpypzA. A related salt was described in the 1980s by Toraya et al.,[14] in which an anionic, but also purely inorganic, Mo^{6+} oxide chain cocrystallizes with dimethylammonium. Therefore, to the best of our knowledge, compound **2** is unique in that it constitutes the first example of an inorganic/organic composite polymer having a purely octahedral Mo^{6+} oxide core. Crystallographic data (excluding structure factors) for **2** have been deposited with the Cambridge Crystallographic Data Centre as No. 865397. Copies of the data can be obtained free of charge via the Internet at http://www.ccdc.cam.ac.uk/conts/retrieving.html or by post at CCDC, 12 Union Road, Cambridge CB2 1EZ, U.K. (fax: 44-1223336033, e-mail: deposit@ccdc.cam.ac.uk).

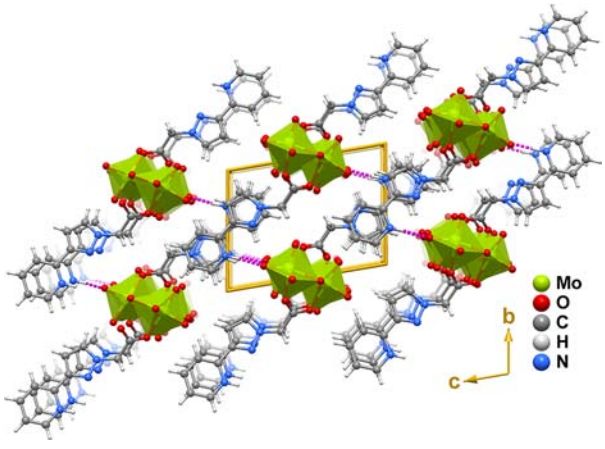

Figure 3. Crystal packing of **2** viewed in perspective along the [100] direction of the unit cell.

An important structural feature which differentiates the composite polymer $_{\infty}^{1}[Mo_2O_6(HpypzA)]$ from those described for related materials concerns the basic building unit of the polymer itself. The asymmetric unit (see Figure S4 in the Supporting Information) is composed of two crystallographically distinct Mo^{6+} metallic centers bridged together by the *syn,syn*-bridging carboxylate group of HpypzA (Figure 2c), leading to a Mo1···Mo2 intermetallic distance of 3.355(1) Å (Figure 2b). The $_{\infty}^{1}[Mo_2O_6(HpypzA)]$ polymer is ultimately

dx.doi.org/10.1021/ic301405r | Inorg. Chem. 2012, 51, 8629−8635

formed by the periodic repetition (through inversion symmetry) of these dinuclear units along the *a* axis of the unit cell, imposing additional Mo1···Mo1^{ii} and Mo2···Mo2^{i} separations of 3.351(1) and 3.338(1) Å, respectively [symmetry codes: (i) *x*, 1 + *y*, *z*; (ii) *x*, *y*, −1 + *z*]. This contrasts with that observed in most of the structures known so far, where inorganic {MoO_4} tetrahedra intercalate in a periodic fashion the hybrid monomers containing the organic ligand (e.g., $[Mo_2O_6(2,2'\text{-bipy})]_n$ and $[Mo_3O_9(2,2'\text{-bipy})_2]_n$[2a]). In $[MoO_3(2,2'\text{-bipy})]_n$, a material which does not contain the aforementioned {MoO_4} tetrahedra, the organic ligands from adjacent monomers are only slightly twisted so as to minimize steric repulsion.[2a] Conversely, in **2**, consecutive HpypzA molecules are exactly located at opposite sites of the inorganic Mo^{6+} oxide core as depicted in Figure 2a.

The coordination environments of the two crystallographically independent Mo^{6+} centers are very similar, each being coordinated to three μ_3-bridging oxide groups, two terminal Mo═O groups, and one oxygen arising from the *syn*,*syn*-bridging carboxylate group of HpypzA. These {MoO_6} coordination environments are distorted octahedra (Figure 2c): while the internal O−Mo−O octahedral *trans* angles are found in the wide range of 149.5(15)−175.7(13)° (amplitude of *ca.* 26.2°), the *cis* angles are instead in the range of 75.0(13)−106.6(16)° (amplitude of *ca.* 31.6°). The Mo−O bond distances range from 1.679(14) to 2.42(3) Å (amplitude of *ca.* 0.74 Å; Table S2). Even though the observed amplitudes for these physical parameters are very large, a search in the CSD for the geometrical parameters of {MoO_6} octahedra showed that the Mo−O bond distances are indeed found in the *ca.* 1.59−2.67 Å window (from 2247 hits in the database). The dispersion in bond angles is even wider, but a significant number of structures start to show O−Mo−O octahedral angles above *ca.* 70°, which agrees well with those observed for compound **2**.

As depicted in Figure 2c, the equatorial planes of the two {MoO_6} octahedra are composed of the three μ_3-bridging oxide groups (O1, O1^{ii}, and O6^{i} for Mo1, and O1, O6, and O6^{i} for Mo2) and one terminal Mo═O group (O3 for Mo1 and O5 for Mo2), with the apical positions being occupied by the *syn*,*syn*-bridging carboxylate group and the remaining terminal Mo═O moieties. The *trans* influence of the latter groups is, remarkably, not very strong: while in compound **2**, the two Mo^{6+} centers are raised from their average equatorial plane by *ca.* 0.16 and 0.29 Å (for Mo1 and Mo2) toward O2 and O4, respectively, a search in the CSD reveals that typical values have a median of *ca.* 0.49 Å.

The close packing of individual $_\infty^1[Mo_2O_6(HpypzA)]$ composite polymers to form the crystal structure of **2** is mediated by a series of supramolecular contacts. The most striking ones arise from the interdigitation of adjacent polymers, which promotes the occurrence of strong onset $\pi-\pi$ contacts connecting adjacent rings of coordinated [3-(pyridinium-2-yl)-1*H*-pyrazol-1-yl]acetate molecules (Figures 3 and 4b): the intercentroid distances range from 3.55(3) to 3.85(3) Å (Table S3) with neighboring rings forming a linear arrangement parallel to the *a* axis of the unit cell. Additionally, the HpypzA molecules are engaged in both strong (N^+−H···O) and weak (C−H···O) hydrogen bonds with oxide groups belonging to adjacent $_\infty^1[Mo_2O_6(HpypzA)]$ polymers (Figure 4a; see Table S3 for geometrical features of these supramolecular contacts). While the latter weak C−H···O contacts (d(C···O) = 2.79−3.32 Å; <(CHO) = 101−160°) essentially

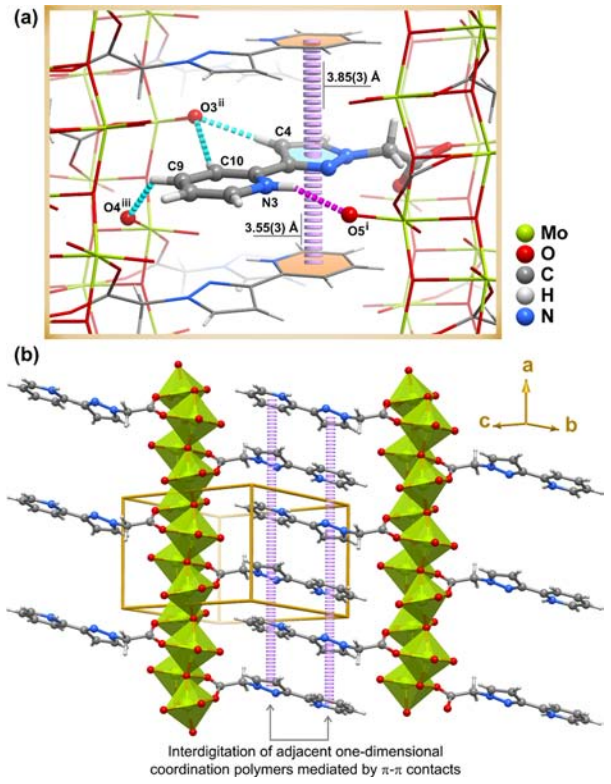

Figure 4. Schematic representation of the supramolecular contacts present in $[Mo_2O_6(HpypzA)]$ (**2**). (a) Chemical environment of the coordinated [3-(pyridinium-2-yl)-1*H*-pyrazol-1-yl]acetate moiety, showing the strong (N^+−H···O, dashed pink line) and weak (C−H···O, dashed light blue lines) supramolecular contacts in which this molecule is engaged with neighboring $_\infty^1[Mo_2O_6(HpypzA)]$ polymers. For geometrical details on the represented supramolecular contacts, see Table S3. Symmetry codes used to generate equivalent atoms: (i) *x*, 1 + *y*, *z*; (ii) *x*, *y*, −1 + *z*; (iii) −*x*, −*y*, −*z*. (b) Close packing of two adjacent $_\infty^1[Mo_2O_6(HpypzA)]$ polymers emphasizing the $\pi-\pi$ contacts between rings of coordinated HpypzA molecules.

occur within the two-dimensional supramolecular layers formed by the aforementioned $\pi-\pi$ contacts, the strong N^+−H···O hydrogen bonds (d(N···O) = 2.88 Å; <(NHO) = 158°) promote effective connections between such layers as depicted in Figure 3.

Catalytic Epoxidation of *cis*-Cyclooctene. The catalytic performance of **2** was investigated in liquid-phase epoxidation using *cis*-cyclooctene (Cy) as a model substrate, TBHP as an oxidant, and, optionally, hexane (hex), decane (dec), 1,2-dichloroethane (DCE), ethanol (EtOH), or water as a cosolvent, at 55 °C. 1,2-Epoxycyclooctane (CyO) was always the only observed reaction product. Without adding a catalyst, the Cy conversion at 24 h was always less than 10%.

The first catalytic reaction with **2** was performed using a decane solution of TBHP as the oxidant source (TBHPdec), without adding a cosolvent, which gave a CyO yield of 57% at 24 h. When decane or hexane were used as a cosolvent, the reaction was sluggish, giving 26% and 24% CyO yield, respectively, at 24 h (Figure 5). A much higher CyO yield (74%) was observed for the more polar cosolvent DCE, which may be partly due to favorable competitive adsorption effects on the catalyst surface. Notably, the polarities of the solvents follow the order (dipole moments measured at 25 °C) DCE (1.8 D) ≫ dec or hex (<0.1 D).[15]

dx.doi.org/10.1021/ic301405r | *Inorg. Chem.* 2012, 51, 8629−8635

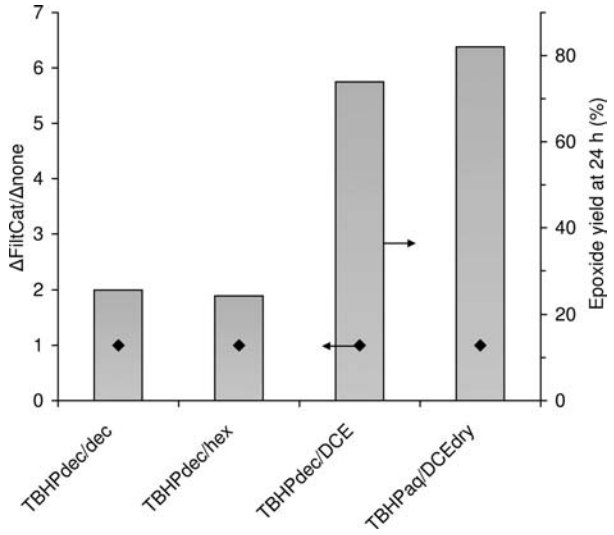

Figure 5. CyO yields and homogeneous catalytic contributions for the epoxidation of Cy at 55 °C using **2** and different oxidant/cosolvent systems (the catalytic reaction is heterogeneous in nature when ΔFiltCat/Δnone = 1; for ΔFiltCat/Δnone > 1, a homogeneous catalytic contribution exists).

All of the tested TBHPdec/cosolvent systems were biphasic liquid (colorless)−solid (L(cl)−S), and it was possible to recover at least 92 wt % of the initial mass of **2** by centrifugation, after a 24 h batch run. The recovered solids possessed the same color as **2** (pale blue), and the respective ATR FT-IR spectra were all alike (exemplified in Figure S5 for the solid recovered from the TBHPdec/DCE system). For all of the tested cosolvents, the Filt_test assay (described in the Experimental Section) gave ΔFiltCat/Δnone ≅ 1, from which it is possible to conclude that the catalytic reaction is heterogeneous in nature (Figure 5). Furthermore, the reused solid gave a comparable CyO yield (80%) to that observed for the fresh catalyst (74%).

When TBHPaq was used as the oxidant solution instead of TBHPdec, CyO yields after 24 h of reaction were 18% when no cosolvent was added, 16% with EtOH, and 32% with water. The reaction mixtures were biphasic L(cl)−S for EtOH and triphasic L(cl)−L(cl)−S for H_2O. More than 80 wt % of the initial mass of **2** could be recovered by centrifugation. The ATR FT-IR spectra of the recovered solids were similar to that of **2** (Figure S5), suggesting that the latter is fairly stable under the applied reaction conditions. These results parallel those observed for the **2**/TBHPdec/cosolvent systems in that the type of cosolvent does not seem to influence the catalyst stability.

In an attempt to couple the attractive catalytic performance (active, stable, heterogeneous bulk catalyst) observed for the **2**/TBHPdec/DCE system with the economic and environmental benefits of using TBHPaq instead of TBHPdec, a mixture of TBHPaq/DCE was predried, followed by the addition of Cy and the catalyst **2**. The resulting system (denoted TBHPaq/DCEdry) gave 82% CyO yield at 24 h, which is far better than that observed for the TBHPaq/cosolvent based systems and slightly better than that observed for the TBHPdec/DCE system (74%). The Filt_test assay performed for the TBHPaq/DCEdry system gave ΔFiltCat/Δnone ≅ 1, suggesting that the catalytic reaction was heterogeneous in nature, which is congruent with that observed for the TBHPdec/DCE system (Figure 5).

When compared with literature data for hybrid oxomolybdenum−organic oligo/polymeric compounds used as bulk heterogeneous catalysts in the same model reaction (with TBHPdec), the catalytic activity of **2** seems much higher than that for $\{[MoO_3(bipy)][MoO_3(H_2O)]\}_n$ (22% CyO yield at 24 h)[6] and lower than those for $[Mo_4O_{12}(pzpy)_4]$ and $[Mo_8O_{24}(pypzEA)_4]$ (92% and 100% CyO yield at 24 h, respectively).[4] The catalyst stability of these materials compare favorably with catalysts prepared by the heterogenization of homogeneous molybdenum catalysts on inorganic or organic−inorganic hybrid mesoporous supports. As noted by Thiel and co-workers in a recent review,[16] supported molecular catalysts based on molybdenum frequently exhibit poor recycling stability; i.e., catalytic activity decreases between recycling runs. The causes of catalyst deactivation include chemical and structural alterations of the catalysts and leaching of active species that are weakly adsorbed/entrapped on the support. Catalyst stabilities are generally very sensitive to the preparation procedures, which are less attractive than that of **2** in that they involve the use of multicomponent reaction mixtures (critical in terms of atom efficiency), whereas **2** is prepared in a straightforward manner in aqueous media using only the precursor complex as a starting material.

■ CONCLUSIONS AND OUTLOOK

With the conclusion of this study, three very distinct and structurally diverse molybdenum oxide/organodiamine compounds have been prepared by the reaction of complexes of the type $[MoO_2Cl_2L]$ with water at 100−120 °C, namely, the polymeric materials $\{[MoO_3(2,2'\text{-bipy})][MoO_3(H_2O)]\}_n$ and (in this work) $[Mo_2O_6(HpypzA)]$ and the octanuclear complex $[Mo_8O_{22}(OH)_4(4,4'\text{-di-}tert\text{-butyl-}2,2'\text{-bipyridine})_4]$; these are active and stable epoxidation catalysts. The compounds are obtained as phase-pure microcrystalline powders in yields of 70−90%. It may be envisaged that the use of other precursor complexes with different ligands and geometries, including chiral derivatives, will lead to the synthesis of multifunctional inorganic/organic molybdenum oxide materials. For $[Mo_2O_6(HpypzA)]$ (**2**), structure solution was only possible through a complex combination of X-ray diffraction techniques and approaches, in conjunction with other physicochemical data. In contrast to the compounds with the bipyridine derivatives, in **2** the ligand is coordinated to the Mo centers via the carboxylate group (formed by *in situ* hydrolysis of the ester group in pypzEA) rather than the N donor atoms, which leads to an interesting structural motif in which outstretched pyrazolylpyridine groups of adjacent polymers interdigitate in a zipper-like fashion through strong $\pi-\pi$ contacts. If the N−N-chelating coordination sites of the pyrazolylpyridine ligands are open to metal insertion, this could lead to materials with a broad range of properties and applications.

■ ASSOCIATED CONTENT

Ⓢ Supporting Information

Detailed description of X-ray diffraction studies, crystallographic information file (CIF), rotational movie showing the one-dimensional $_\infty{}^1[Mo_2O_6(HpypzA)]$ polymer, graphical representation of the asymmetric unit in **2**, representative SEM images of bulk microcrystalline **2**, and ATR FT-IR spectra of **1**, **2**, and solids recovered from catalytic runs. This material is available free of charge via the Internet at http://pubs.acs.org.

dx.doi.org/10.1021/ic301405r | *Inorg. Chem.* 2012, 51, 8629−8635

AUTHOR INFORMATION

Corresponding Author

*E-mail: filipe.paz@ua.pt; igoncalves@ua.pt.

Notes

The authors declare no competing financial interest.

ACKNOWLEDGMENTS

We are grateful to the *Fundação para a Ciência e a Tecnologia* (FCT), COMPETE, and the European Union for funding through the R&D project No. PDTC/QUI-QUI/098098/2008 (FCOMP-01-0124-FEDER-010785). The FCT is acknowledged for financial support towards the purchase of the single-crystal diffractometer, for Ph.D. grants to S.F. (SFRH/BD/45116/2008) and T.R.A. (SFRH/BD/64224/2009), and for a postdoctoral grant to P.N. (SFRH/BPD/73540/2010). We appreciate the continued support from the Associate Laboratory CICECO (Pest-C/CTM/LA0011/2011).

REFERENCES

(1) (a) Hagrman, P. J.; Hagrman, D.; Zubieta, J. *Angew. Chem., Int. Ed.* **1999**, *38*, 2638. (b) Hagrman, D.; Hagrman, P. J.; Zubieta, J. *Comments Inorg. Chem.* **1999**, *21*, 225.

(2) (a) Zapf, P. J.; Haushalter, R. C.; Zubieta, J. *Chem. Mater.* **1997**, *9*, 2019. (b) Kim, J.; Lim, W. T.; Koo, B. K. *Inorg. Chim. Acta* **2007**, *360*, 2187. (c) Lu, Y.; Wang, E.; Yuan, M.; Li, Y.; Hu, C. *J. Mol. Struct.* **2003**, *649*, 191. (d) Hagrman, P. J.; LaDuca, R. L., Jr.; Koo, H.-J.; Rarig, R., Jr.; Haushalter, R. C.; Whangbo, M.-H.; Zubieta, J. *Inorg. Chem.* **2000**, *39*, 4311. (e) Cui, C.-P.; Dai, J.-C.; Du, W.-X.; Fu, Z.-Y.; Hu, S.-M.; Wu, L.-M.; Wu, X.-T. *Polyhedron* **2002**, *21*, 175. (f) Niu, J.; Wang, Z.; Wang, J. *Inorg. Chem. Commun.* **2004**, *7*, 556. (g) Xu, Y.; Lu, J. *Inorg. Chim. Acta* **1999**, *295*, 222. (h) Zapf, P. J.; LaDuca, R. L., Jr.; Rarig, R. S., Jr.; Johnson, K. M., III; Zubieta, J. *Inorg. Chem.* **1998**, *37*, 3411. (i) LaDuca, R. L., Jr.; Rarig, R. S., Jr.; Zapf, P. J.; Zubieta, J. *Inorg. Chim. Acta* **1999**, *292*, 131. (j) Zhou, Y.; Zhang, L.; Fun, H.-K.; You, X. *Inorg. Chem. Commun.* **2000**, *3*, 114. (k) Li, D.; Liu, Y.; Wei, P.; Hu, B.; Zhang, X. *Acta Crystallogr., Sect. E: Struct. Rep. Online* **2009**, *E65*, m1074. (l) Xu, Y.; Lu, J.; Goh, N. K. *J. Mater. Chem.* **1999**, *9*, 1599. (m) Rarig, R. S., Jr.; Zubieta, J. *Inorg. Chim. Acta* **2001**, *312*, 188. (n) Chuang, J.; Ouellette, W.; Zubieta, J. *Inorg. Chim. Acta* **2008**, *361*, 2357. (o) Lysenko, A. B.; Senchyk, G. A.; Lincke, J.; Lässig, D.; Fokin, A. A.; Butova, E. D.; Schreiner, P. R.; Krautscheid, H.; Domasevitch, K. V. *Dalton Trans.* **2010**, *39*, 4223. (p) Hagrman, D.; Zubieta, C.; Rose, D. J.; Zubieta, J.; Haushalter, R. C. *Angew. Chem., Int. Ed. Engl.* **1997**, *36*, 873. (q) Zapf, P. J.; Warren, C. J.; Haushalter, R. C.; Zubieta, J. *Chem. Commun.* **1997**, 1543. (r) Hagrman, D.; Zapf, P. J.; Zubieta, J. *Chem. Commun.* **1998**, 1283. (s) Hagrman, D.; Sangregorio, C.; O'Connor, C. J.; Zubieta, J. *J. Chem. Soc., Dalton Trans.* **1998**, 3707. (t) Hagrman, P. J.; Zubieta, J. *Inorg. Chem.* **2000**, *39*, 5218. (u) Rarig, R. S., Jr.; Lam, R.; Zavalij, P. Y.; Ngala, J. K.; LaDuca, R. L., Jr.; Greedan, J. E.; Zubieta, J. *Inorg. Chem.* **2002**, *41*, 2124. (v) Kong, Z.; Weng, L.; Tan, D.; He, H.; Zhang, B.; Kong, J.; Yue, B. *Inorg. Chem.* **2004**, *43*, 5676. (w) Coué, V.; Dessapt, R.; Bujoli-Doeuff, M.; Evain, M.; Jobic, S. *Inorg. Chem.* **2007**, *46*, 2824. (x) Yang, M.-X.; Chen, L.-J.; Lin, S.; Chen, X.-H.; Huang, H. *Dalton Trans.* **2011**, *40*, 1866.

(3) Amarante, T. R.; Neves, P.; Coelho, A. C.; Gago, S.; Valente, A. A.; Paz, F. A. A.; Pillinger, M.; Gonçalves, I. S. *Organometallics* **2010**, *29*, 883.

(4) Neves, P.; Amarante, T. R.; Gomes, A. C.; Coelho, A. C.; Gago, S.; Pillinger, M.; Gonçalves, I. S.; Silva, C. M.; Valente, A. A. *Appl. Catal. A: Gen.* **2011**, *395*, 71.

(5) Sanchez, C.; Belleville, P.; Popall, M.; Nicole, L. *Chem. Soc. Rev.* **2011**, *40*, 696.

(6) Abrantes, M.; Amarante, T. R.; Antunes, M. M.; Gago, S.; Paz, F. A. A.; Margiolaki, I.; Rodrigues, A. E.; Pillinger, M.; Valente, A. A.; Gonçalves, I. S. *Inorg. Chem.* **2010**, *49*, 6865.

(7) Amarante, T. R.; Neves, P.; Tomé, C.; Abrantes, M.; Valente, A. A.; Paz, F. A. A.; Pillinger, M.; Gonçalves, I. S. *Inorg. Chem.* **2012**, *51*, 3666.

(8) Bruno, S. M.; Pereira, C. C. L.; Balula, M. S.; Nolasco, M.; Valente, A. A.; Hazell, A.; Pillinger, M.; Ribeiro-Claro, P.; Gonçalves, I. S. *J. Mol. Catal. A: Chem.* **2007**, *261*, 79.

(9) Bruno, S. M.; Fernandes, J. A.; Martins, L. S.; Gonçalves, I. S.; Pillinger, M.; Ribeiro-Claro, P.; Rocha, J.; Valente, A. A. *Catal. Today* **2006**, *114*, 263.

(10) (a) Favre-Nicolin, V.; Cerny, R. *FOX - A Program for ab initio Structure Solution from Powder Diffraction Data*; Swiss National Science Foundation, University of Geneva: Geneva, Switzerland, 2000. (b) Favre-Nicolin, V.; Cerny, R. *J. Appl. Crystallogr.* **2002**, *35*, 734.

(11) (a) Deacon, G. B.; Phillips, R. J. *Coord. Chem. Rev.* **1980**, *33*, 227. (b) Nakamoto, K. *Infrared and Raman Spectra of Inorganic and Coordination Compounds*, 4th ed.; J. Wiley & Sons: New York, 1986. (c) Robert, V.; Lemercier, G. *J. Am. Chem. Soc.* **2006**, *128*, 1183. (d) Nara, M.; Torii, H.; Tasumi, M. *J. Phys. Chem.* **1996**, *100*, 19812.

(12) (a) Modec, B.; Dolenc, D.; Kasunič, M. *Inorg. Chem.* **2008**, *47*, 3625. (b) Shirai, M.; Arai, M.; Murakami, K. *Energy Fuels* **1999**, *13*, 465. (c) Baggio, R.; Garland, M. T.; Pirec, M. *J. Chem. Soc., Dalton Trans.* **1996**, 2747.

(13) (a) Allen, F. H. *Acta Crystallogr., Sect. B: Struct. Sci.* **2002**, *58*, 380. (b) Allen, F. H.; Motherwell, W. D. S. *Acta Crystallogr., Sect. B: Struct. Sci.* **2002**, *58*, 407.

(14) Toraya, H.; Marumo, F.; Yamase, T. *Acta Crystallogr., Sect. B: Struct. Sci.* **1984**, *40*, 145.

(15) (a) Reid, R. C.; Prausnitz, J. M.; Poling, B. E. *The Properties of Gases and Liquids*, 4th ed.; McGraw-Hill: New York, 1987. (b) Hayes, B. L. *Microwave Synthesis: Chemistry at the Speed of Light*; CEM Publishing: Matthews, NC, 2002.

(16) Shylesh, S.; Jia, M.; Thiel, W. R. *Eur. J. Inorg. Chem.* **2010**, 4395.